Development of a Bipedal Robot with Genetic Algorithm Based Motion Control

(article starts on next page)

DEVELOPMENT OF A BIPEDAL ROBOT WITH GENETIC ALGORITHM BASED MOTION CONTROL

Hans Sandholt, Jimmy Pettersson, Mattias Wahde

Division of Mechatronics,
Department of Machine and Vehicle Systems,
Chalmers University of Technology
SE-412 96 Göteborg, Sweden
e-mail:
hans.sandholt@me.chalmers.se,
jimmy.pettersson@me.chalmers.se,
mattias.wahde@me.chalmers.se

Abstract

A description of the development of a bipedel robot currently under development at the Division of Mechatronics at Chalmers University of Technology is given. Furthermore, we introduce a method, based on genetic algorithms in conjunction with neural networks, for robust posture control for bipedal robots. We also present some early results from simulations using this method. Finally, a preliminary design of a force and torque sensor for posture control is described and the results of a hardware validation test are presented.

1 Introduction

During the last few years, bipedal robots have evolved from being a remote possibility for the future to being a reality for the present. Around the world, and particularly in Japan, there are now a large number of projects dealing with bipedal and humanoid robotics (Wahde and Pettersson, 2002). While most of these projects are carried out in an academic setting, there also exists commercially oriented projects (such as Honda's ASIMO, Sony's SDR-3X etc.).

In 2001, a humanoid project was initiated at the Division of Mechatronics at Chalmers University of Technology in Göteborg, Sweden. In our research group, we emphasize the use of biologically inspired computation methods for many aspects of the development of bipedal robots.

We are currently constructing a bipedal robot, which represents the first stage in our development of a complete humanoid robot. The aim of this paper is to describe the proposed biped, and also to introduce the control method, which is based on genetic algorithms. The method makes use of control signals (such as e.g. the pressure distribution under the feet) similar to those available in biological systems.

Group id	Name	DOF
001	Foot	
002	Ankle	2
003	Lower leg	
004	Knee	1
005	Upper leg	
006	Hip joint	3
007	Hip	
008	Spine joint	3

Table 1: Groups defining the bipedal robot and degrees of freedom (DOF) per part where applicable.

We will present the results of simulations aimed at evolving a controller for maintaining an upright posture in the presence of perturbations. In addition, we will discuss, in some detail, the hardware implementation of a robot foot equipped with force sensors.

This paper contains two main parts: first, in Sect. 2 a rather detailed description of the proposed bipedal robot is given. Second, in Sect. 3 we describe the algorithms, simulations, hardware, and preliminary results for our investigation concerning the evolution of posture control. Some conclusions are given in Sect. 4.

2 Outline of the bipedal robot hardware architecture

The parts of the robot are grouped according their locations within the robot, e.g. foot, lower leg, knee, etc. In total the complete humanoid robot is divided into 19 groups, of which 8 are needed to describe the bipedal robot. These groups are listed in Table 1. Each group consists of both mechanical and electrical parts such as motors, gears, sensors, electronics, power electronics, etc. These components are not described in detail in this paper. Instead, the description is limited to an outline of the general structure and motivation for some of the choices made during the design process.

The main goal with the hardware design of this robot was to arrive at a robust, low cost design with low weight, and with a mobility range as close as possible to that of a human. The robot will have 15 DOF in order to be able to mimic the motion pattern of human gait. These DOFs are distributed according to Table 1.

2.1 Actuators

It is of great importance to have high power density in the actuators in order to avoid excessive mass. Therefore, actuators have been combined into generating motions using combined and differential drive. This design is implemented in the foot motion and in the sagittal and frontal motion of the leg. The configuration of a foot is illustrated in the left panel of Fig. 1.

Furthermore, Teflon coated slide bearings have been chosen because of their low weight and low static friction. The latter is essential when performing small, smooth motions while at the same time avoiding excessive torque and high demands on the motion control system.
The transformation from rotating to linear motion is performed using lead screws with

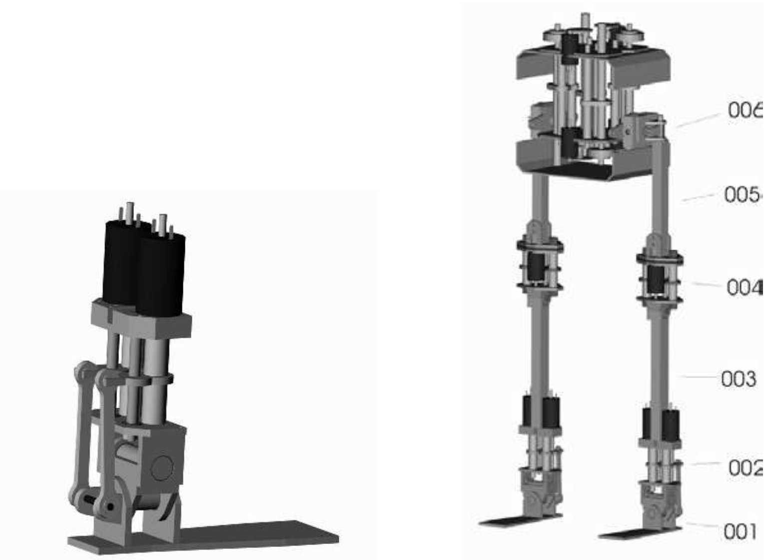

Figure 1: Left panel: Foot actuator demonstrating the combination of two motors used for gaining high power density. The two motors run in parallel and differential mode to generate high torque, depending on the set motion. Right panel: Rendered bipedal robot with group indicators.

plastic nuts. The motivation for this choice was low cost, low weight, and low static friction.

Developing a bipedal robot is a challenging task with high demands on concurrent engineering. At present, we are evaluating the knee actuator of the biped with respect to smooth mechanical actuation and general performance. The knee actuator is shown in Figure 2.

2.2 Joints

All joints are designed to be as compact and light as possible without requiring high tensions and strains. The joints are equipped with Teflon coated slide bearings with the same motivation as for the actuator (see above).

2.3 Sensors

The bipedal robot is equipped with several sensors that are currently under evaluation. For example, the joints are, at present, equipped with potentiometers for reading the angular position, but incremental and absolute encoders are also being considered.

The feet of the robot will be equipped with several strain gauge sensors in order to measure the torque and force distribution under each foot. A more complete discussion of these sensors is given in Sect. 3.2

Figure 2: The knee actuator showing the motor in the background and the moving plate in the foreground. The gearbox is hidden inside the top housing.

2.4 Electronics

Each actuator is driven and controlled by a Power Drive Unit (PDU) containing both the power drive module and actuator sensor interface, e.g. electrical signal conditioning circuitry. The motor drive is realized using high-performing PWM driver, LMD18200 from National semiconductor, whose circuits are capable of delivering 75 W continuously and 150 W momentarily. Each PDU is connected to a Motor Control Unit (MCU), responsible for the low-level control such as PWM-signal generation, actuator monitoring, and closing the low-level motor control loop. The MCU is connected to the higher control system, running on an external PC, using a 1Mbit CAN-bus interface. A schematic view of the electronic modules is shown in Fig. 3.

3 Posture control and walking

Several methods for generating dynamically stable bipedal walking patterns have been suggested in the literature. A common approach is to base the control method on the position of the zero-moment point (ZMP), see e.g. Arakawa and Fukuda (1996). The ZMP is a generalization of the centre-of-mass, and was originally introduced by Vukobratovic and Juricic (1969). Simply expressed, the ZMP condition states that the robot will maintain an upright posture as long as the ZMP resides within the convex hull of the support area defined by the supporting foot (or feet, in the double-support phase).

Using the ZMP criterion, there are two main approaches to the generation of bipedal gaits (Huang, Nakamura and Inamura, 2001). In the first approach, it is assumed that the environment is well known, and the bipedal gait is generated off-line and is then applied to the robot (Hirai, Hirose, Haikawa and Takenaka, 1998). In the second approach, an on-line controller determines the torques required to keep the ZMP in position (Fujimoto and Kawamura, 1998).

The ultimate aim of humanoid robotics is to generate robots that are able to function in a large variety of environments, and to cope with unexpected situations. Clearly, to realize this aim, it is not enough to use e.g. pre-defined trajectories for locomotion. In addition, control algorithms based on classical control are often computationally

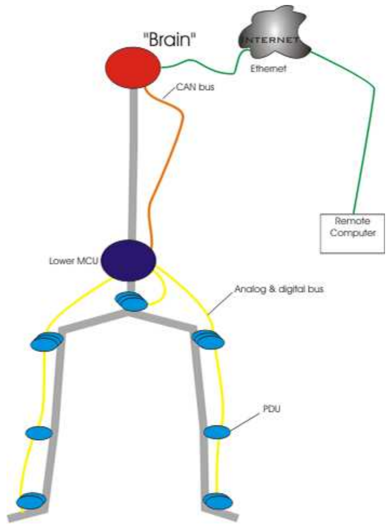

Figure 3: Schematic drawing over the electronic modules and the buses used. Each actuator is driven by a PDU and up to 16 PDU:s are controlled by a MCU. The MCU is connected to a higher control system referred to as ”Brain” in the drawing.

expensive. This is not to say that such controllers should not be used in humanoid robots. On the contrary, for the low-level control regulating e.g. individual actuators such methods are certainly appropriate.

However, for the high-level control of walking, we believe that alternative methods should be explored. Humanoid robots are inspired by biological systems, and therefore it makes sense to attempt to use methods for optimization and adaptation similar to those found in nature. One such method, which will be used in this paper, is genetic algorithms (GAs) (See e.g. Mitchell 1996). GAs have been used in several investigations concerning bipedal robots, see e.g. Arakawa and Fukuda (1996), Cheng and Lin (1995) and Paul and Bongard (2001).

An important feature of genetic algorithms, which we believe has yet to be fully exploited in bipedal robotics research, is their ability to optimize not only the parameters but also the structure of the control system under study (Pettersson, Sandholt and Wahde, 2001). This is an important feature in complex problems for which it may be difficult to derive an analytical model, or for which the use of the analytical model is computationally expensive.

In this study, we have used a genetic algorithm in order to study a simplified aspect of bipedal motion, namely the ability to maintain an upright posture in the presence of external perturbations, using only the pressure distribution under the feet as input signals. The use of the foot pressure distribution is motivated by the fact that it is a signal that is readily available to biological walking systems, i.e. humans or animals.

Our study has, so far, been limited to one-legged balancing, corresponding to the single-support phase of bipedal locomotion. Furthermore, we have only considered the balancing of a rigid foot on a flat surface, for which the pressure distribution under the foot can be determined using much fewer pressure sensors than would be needed for a deformable foot or for rugged surfaces.

In principle, a control system for balancing could be evolved directly in hardware, i.e. without using simulations. Such an approach has been used by e.g. Wolff and

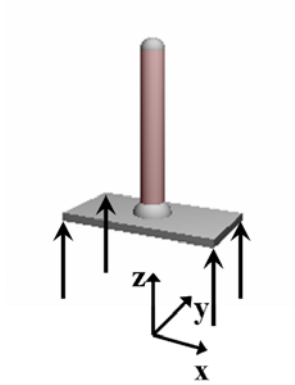

Figure 4: The setup used in the posture control simulations.

Nordin (2001). However, when performing both parametric and structural optimization of a control system, a very large number of candidate solutions must be evaluated, making evolution in hardware too time-consuming. Furthermore, if the GA is implemented in the hardware, the system must be monitored continuously, in order to replace worn out parts etc. (Wolff and Nordin, 2001).

Thus, we have chosen to implement the GA in simulation. We will begin by discussing the simulations, and will then briefly describe a hardware implementation of a foot equipped with pressure sensors.

3.1 Posture control simulations

The simulation code was written in Delphi (Object-oriented pascal). The Delphi environment allows rapid development of Windows software, and its speed is comparable to that of C++.

Simulation setup The simulated system, which is shown in Fig. 4, consists of a massless pole with a pointlike weight (representing the upper body and swing leg of the robot) attached to a foot plate which, in turn, is connected to the ground via 4 spring-damper systems, one at each corner of the foot plate. The leg is modelled as an inverted spherical pendulum with the addition of a vertical acceleration component due to the motion of the foot plate. The motion of the foot plate is given by

$$m\ddot{z} = \sum_{i=1}^{4} F_i - mg - R_z \quad (1)$$

$$I\alpha = \tau + \sum_{i=1}^{4} r_i \times F_i \quad (2)$$

where $\ddot{z}$ is the vertical acceleration of the foot, α is the vector of angular accelerations, F_i is the force from the i^{th} spring/damper pair, R_z is the vertical component of the reaction force exerted by the inverted pendulum, τ is the vector of applied torques in the horizontal plane, I is the moment of inertia, and r_i is the location vector of the i^{th} force F_i. We have made the assumption that the friction under the foot plate is sufficient to keep it from moving in the horizontal direction. Forces from the four spring/damper pairs were calculated as

$$F_i = -K_s \Delta z_i - K_d v_i \quad , i = 1,2,3,4 \tag{3}$$

where K_s is the spring constant, K_d the damping coefficient, Δz_i the spring contraction, and v_i the velocity of the connection points of the i^{th} damper. With this setup, there can be no forces pulling the foot down. Thus, negative forces F_i were set to zero.

The spherical pendulum is assumed to be actuacted by two joints that deliver torques in the $x-$ and $y-$directions (measured relative to the foot plate), respectively.

In the simulations, the dimensions of the foot plate were 0.3m (length) and 0.1m (width). The weight of the foot plate was set to 1 kg and the weight and length of the leg were set to 5 kg and 0.80m, respectively. The spring constants and damping coefficients were 1000 N/m and 50 Ns/m, respectively. The perturbation torques were of order 1 Nm.

Control system architecture In keeping with our aim to develop a biologically inspired high level robot control system, we chose to use a neural network architecture for our simulations.

Initially a simple feedforward network was tried. This network had four input nodes, one for each of the four force sensors attached to the foot plate, see Fig. 4, and two outputs representing the torques (τ_x and τ_y) of the leg actuators.

Perturbations were simulated by adding a small amount to the torque generated by the neural network as

$$\epsilon_x = \alpha_1 \cos(\beta_1 t) + \gamma_1 \sin(\delta_1 \sqrt{2} t) \tag{4}$$
$$\epsilon_y = \alpha_2 \cos(\beta_2 t) + \gamma_2 \sin(\delta_2 \sqrt{2} t) \tag{5}$$

where $\{\alpha_i, \beta_i, \gamma_i, \delta_i\}$ are constants. The total applied torque (τ'_x and τ'_y) was then set as

$$\begin{pmatrix} \tau'_x \\ \tau'_y \\ 0 \end{pmatrix} = \begin{pmatrix} \tau_x + \epsilon_x \\ \tau_y + \epsilon_y \\ 0 \end{pmatrix} \tag{6}$$

The weights of the neural network were determined using a genetic algorithm with tournament selection and generational replacement of individuals. The fitness measure was taken essentially as the integrated inverse of the deviation from the desired posture, which taken as the position corresponding to a 10 degree rotation around the $y-$axis.

Preliminary results The simple feedforward network architecture turned out to be too simple to generate useful results: the leg suffered divergent oscillations which ultimately caused it too fall.

In order to improve the balancing of the leg, a continuous-time recurrent neural network (RNN) architecture was chosen instead. In this architecture, each neuron is connected to all other neurons (including itself), and the dynamic equations for neuron i take the form

$$\tau_i \dot{x}_i + x_i = \sigma\left(\Sigma_{j=1}^{N} w_{ij} x_j + I_i\right), \quad i = 1, \ldots, N \tag{7}$$

where x_i denotes the output from neuron i, and w_{ij} are the weights connecting neuron j to neuron i. σ is a sigmoidal squashing function, here chosen as

$$\sigma(z) = \tanh(bz), \tag{8}$$

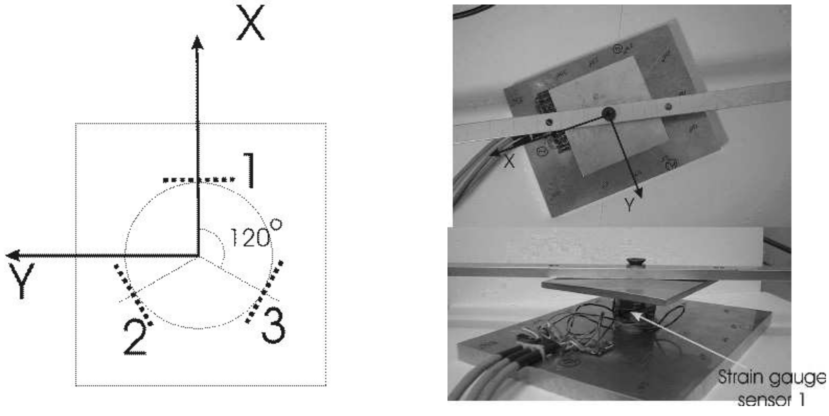

Figure 5: Left panel: Schematic drawing of a foot sensor. Right panel: The evaluation module of the foot sensor. In the upper part of the figure the module is shown from above. The coordinate system is superimposed on the picture and the numbering of the sensors is, from the x-axis 1,2, and 3, with 120 degrees relative angular displacement.

where b is a constant. The external input I_i is equal to 0 at all times except for the four input neurons which read the four force values $F_k, \quad k = 1, \ldots, 4$. The output torques are taken as the output values from two selected neurons, multiplied by a scale factor. The τ_i are time constants, which provide the network with a primitive form of memory (something which the simple feedforward network lacks).

With this network architecture, better results were obtained: the best networks obtained by the genetic algorithm were able to balance the leg for the complete duration of the simulation.

3.2 Haptic foot sensor hardware

Guided by the results of our simulations, we are evaluating ground contact (foot) sensors, which are based on strain gauge sensors. The basic idea of the sensor is to use a small cylindrical body, approximately 20 mm in diameter, and to glue three strain gauge sensors with 120 degrees relative angular displacement. A sketch of the arrangement is shown in left panel of Fig. 5 and the current test sensor is shown in the right panel of the same figure.

The transformation of the strain gauge sensor readings into force and torque values is easy to develop analytically. Letting $\delta = (s_1, s_2, s_3)^{\mathrm{T}}$ denote the vector with the sensor readings s_i and $M = (F_z, M_x, M_y)^{\mathrm{T}}$ the vector with the calculated force and torques, we obtain the simple relationship

$$M = T\delta \tag{9}$$

where T is the transformation matrix given by the geometrical relations according to

$$T = E \begin{pmatrix} \frac{1}{3} & \frac{1}{3} & \frac{1}{3} \\ 0 & r\sin\frac{2\pi}{3} & r\sin\frac{4\pi}{3} \\ -r & r\sin\frac{\pi}{6} & r\sin\frac{\pi}{6} \end{pmatrix} \tag{10}$$

where r is the radius of the sensor body and E is a scale factor essentially depending on the Young's modulus of the aluminum cylinder. However, this equation relies on

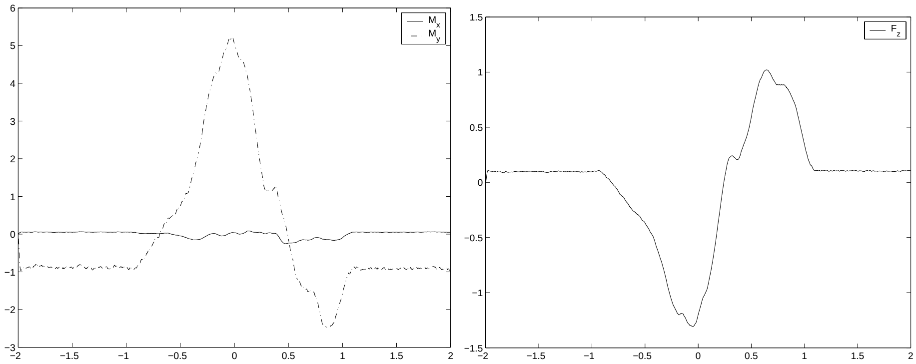

Figure 6: Recorded foot sensor data from one step on a sensor. The recorded step is a normal, slow, step by a 90 kg man. Left Panel: torques, Right Panel: vertical force.

idealized behavior of the sensor. In order to arrive at a more reliable result, it is better to calculate a least square approximation of T based on calibration data, i.e. simultaneous measurements of forces, torques, and deformations.

Hardware validation test A small test with a foot sensor was performed. The test was to take one walking step on the sensor and sample the readings for evaluation using the calculated T matrix.

The recorded step was a normal, slow step performed by a 90 kg man. From the left panel of Fig. 6 it is evident that the torque in the y-direction from walking on the sensor is very clear and that there is almost no torque in the x-direction, as expected.

The calculated vertical force F_z is shown in the right panel of Fig. 6. The measured positive force towards the end of the step is likely to be caused by tensions induced due to the method used for mounting the cylinder. We are currently investigating this issue further.

4 Discussion and Conclusion

The preliminary results from our simulations indicate the importance of choosing an adequate architecture for the control system. The introduction of a recurrent neural network, with its (albeit limited) memory of recent events generated significant improvements in the simulation results. While such networks are more difficult to analyze than ordinary feedforward networks, their advantages easily outweigh this disadvantage. The next step in our analysis will be to allow structural optimization (e.g. variation of the number of neurons) of the neural network during a run of the genetic algorithm.

The initial test done with the foot sensor was promising and indicates good possibilities for future use in the design of a more elaborate haptic foot sensor. A complete foot sensor matrix, consisting of several strain sensors, will be able to sense uneven ground, slopes and even vibration from the ground contact. The latter is of importance for the detection of horizontal slip. However, the test shows that, in its present implementation, the force reading is not yet fully reliable. Additional evaluation and development will lead to changes in the structure of the sensor body and the method of assembly of the sensor. Furthermore, the strain gauge sensor signal is very noisy, and this will put high demands on signal conditioning such as low pass filtering etc.

Acknowledgement

This project is financed in part by the school of Mechanical and Vehicular Engineering at Chalmers University of Technology and Chalmers Center for Mechatronics and System Engineering (CHASE).

References

Arakawa, T. and Fukuda, T. (1996). Natural motion trajectory generation of biped locomotion robot using genetic algorithm through energy optimization, *In: Proc. of the 1996 IEEE International Conference on Systems, Man and Cybernetics* pp. 1495–1500.

Cheng, M.-Y. and Lin, C.-S. (1995). Genetic algorithm for control design of biped locomotion, *In: Proc. of the IEEE International Conference on Robotics and Automation* pp. 1315–1320.

Fujimoto, Y. and Kawamura, A. (1998). Simulation of an autonomous biped walking robot including environmental force interaction, *IEEE Robotics and Automation Magazine* **5**(2): 33–42.

Hirai, K., Hirose, M., Haikawa, Y. and Takenaka, T. (1998). The development of the honda humanoid robot, *In: Proc. of the 1998 IEEE Int. Conf. on Robotics and Automation*.

Huang, Q., Nakamura, Y. and Inamura, T. (2001). Humanoids walk with feedforward dynamic pattern and feedback sensory reflection, *In: Proc. of the IEEE International Conference on Robotics and Automation* pp. 4220–4225.

Mitchell, M. (1996). *An Introduction to Genetic Algorithms*, MIT Press, Cambridge, MA.

Paul, C. and Bongard, J. (2001). The road less travelled: Morphology in the optimization of biped robot locomotion, *In: Proc. of the IEEE/RSJ International Conference on Intelligent Robots and Systems (IROS2001)*.

Pettersson, J., Sandholt, H. and Wahde, M. (2001). A flexible evolutionary method for the generation and implementation of behaviors in humanoid robots, *In: Proc. of the IEEE-RAS International Conference on Humanoid Robots* pp. 279–286.

Vukobratovic, M. and Juricic, D. (1969). Contribution to the synthesis of biped gait, *IEEE. Trans. Bio-Med. Eng.* **BME-16**(1): 1–6.

Wahde, M. and Pettersson, J. (2002). A brief review of bipedal robotics research, *In: Proc. of the 8th Mechatronics Forum International Conference*.

Wolff, K. and Nordin, P. (2001). Evolution of efficient gait with humanoids using visual feedback, *In: Proc. of the IEEE-RAS International Conference on Humanoid Robots* pp. 99–106.